

Crystallographic and FTIR Spectroscopic Evidence of Changes in Fe Coordination Upon Reduction of the Active Site of the Fe-Only Hydrogenase from *Desulfovibrio desulfuricans*

Yvain Nicolet,[§] Antonio L. de Lacey,[†] Xavier Vernède,[§] Victor M. Fernandez,[†]
E. Claude Hatchikian,[‡] and Juan C. Fontecilla-Camps^{*,§}

Contribution from the Laboratoire de Cristallographie et Cristallogénèse des Protéines, Institut de Biologie Structurale, 'J.-P. Ebel' CEA-CNRS, 41, rue Jules Horowitz, 38027 Grenoble, Cedex 1, France, Instituto de Catálisis, CSIC, Campus Universidad Autónoma, 28049 Madrid, Spain, Bioénergétique et Ingénierie des Protéines, Institut de Biologie Structurale et Microbienne, CNRS, 31, chemin Joseph Aiguier, 13402 Marseille, Cedex 20, France.

Received June 12, 2000

Abstract: Fe-only hydrogenases, as well as their NiFe counterparts, display unusual intrinsic high-frequency IR bands that have been assigned to CO and CN⁻ ligation to iron in their active sites. FTIR experiments performed on the Fe-only hydrogenase from *Desulfovibrio desulfuricans* indicate that upon reduction of the active oxidized form, there is a major shift of one of these bands that is provoked, most likely, by the change of a CO ligand from a bridging position to a terminal one. Indeed, the crystal structure of the reduced active site of this enzyme shows that the previously bridging CO is now terminally bound to the iron ion that most likely corresponds to the primary hydrogen binding site (Fe2). The CO binding change may result from changes in the coordination sphere of Fe2 or its reduction. Superposition of this reduced active site with the equivalent region of a NiFe hydrogenase shows a remarkable coincidence between the coordination of Fe2 and that of the Fe ion in the NiFe cluster. Both stereochemical and mechanistic considerations suggest that the small organic molecule found at the Fe-only hydrogenase active site and previously modeled as 1,3-propanedithiolate may, in fact, be di-(thiomethyl)-amine.

Introduction

Hydrogen metabolism in microorganisms is mostly mediated by two types of metalloproteins: NiFe¹ and Fe-only² hydrogenases. The two classes of enzymes are genetically unrelated and, consequently, they represent two independently evolved mechanisms for the biological uptake or production of hydrogen according to the reaction: H₂ ↔ 2 H⁺ + 2 e⁻.³ It has been shown that the first step in the uptake process is the heterolytic cleavage of hydrogen⁴ and that a hydrogen species, probably a hydride, is transiently bound to the active site during turnover.⁵ NiFe hydrogenases have been extensively studied genetically,⁶ spectroscopically,⁷ crystallographically,⁸ and through theoretical calculations.⁹ Nevertheless, the roles of the active site Ni and Fe centers during catalysis remain unclear. A remarkable observation is the fact that the Fe ion is low-spin ferrous with CO and CN⁻ coordination and remains redox inactive throughout the catalytic cycle.¹⁰ In agreement with these results, quantum mechanical calculations indicate that in models for the

various EPR-detectable paramagnetic species, the unpaired electron spin resides mostly at the Ni center.^{9b,c} It has been determined that in most aerobically oxidized enzymes, there is a putative (hydro)oxo ligand asymmetrically bridging the two metal centers (it is closer to Ni than to Fe)^{8b} except for the NiFe hydrogenase from *Desulfovibrio vulgaris*, in which this

(6) (a) Fauque, G.; Peck, H. D., Jr.; Moura, J. J. G.; Huyinh, B. H.; Berlier, Y.; DerVartanian, D. V.; Teixeira, M.; Przybyla, A. E.; Lespinat, P. A.; Moura, I.; LeGall, J. *FEMS Microbiol. Rev.* **1988**, *54*, 299–344. (b) Lutz, S.; Jacobi, A.; Schlensog, V.; Böhm, R.; Sawers, G.; Böck, A. *Mol. Microbiol.* **1991**, *5*, 123–135. (c) Przybyla, A. E.; Robbins, J.; Menon, N.; Peck, H. D., Jr. *FEMS Microbiol. Rev.* **1992**, *88*, 109–135. (d) Wu, L. F.; Mandrand, M. A. *FEMS Microbiol. Rev.* **1993**, *104*, 243–269 (e) Friedrich, B.; Schwartz, E. *Annu. Rev. Microbiol.* **1993**, *47*, 351–383. (f) Hahn, D.; Kueck, U. *Process Biochem.* **1994**, *29*, 633–641. (g) Elsen, S.; Colbeau, A.; Vignais, P. M. *J. Bacteriol.* **1997**, *179*, 968–971. (h) Ruiz-Argueso, T.; Imperial, J.; Palacios, J. M. In *Prokaryotic Nitrogen Fixation: A Model for the Analysis of aBiological Process*; E. W. Triplett, Ed.; Horizon Scientific Press: Wymondhan, U. K., 2000; pp 489–507.

(7) (a) Cammack, R.; Fernandez, V. M.; Schneider, K. In *Bioinorganic Chemistry of Nickel*; J. R. Lancaster, Jr., Ed.; VCH: New York, 1988; Chapter 8. (b) Moura, J. J. G.; Teixeira, M.; Moura, I.; LeGall, J. In *Bioinorganic Chemistry of Nickel*; J. R. Lancaster, Jr., Ed.; VCH: New York, 1988; Chapter 9. (c) Bastian, N. R.; Wink, D. A.; Wackett, L. P.; Livingston, D. J.; Jordan, L. M.; Fox, J.; Orme-Johnson, W. H.; Walsh, C. T. In *Bioinorganic Chemistry of Nickel*; J. R. Lancaster, Jr., Ed.; VCH: New York, 1988; Chapter 10. (d) Bayinka, C.; Whitehead, J. P.; Maroney, M. J. *J. Am. Chem. Soc.* **1993**, *115*, 3576–3585. (e) Bagley, K. A.; Duin, E. C.; Roseboom, W.; Albracht, S. P. J.; Woodruff, W. H. *Biochemistry* **1995**, *34*, 5527–5535. (f) Gu, Z.; Dong, J.; Allan, C. B.; Choudhury, S. B.; Franco, R.; Moura, J. J. G.; Moura, I.; LeGall, J.; Przybyla, A. E.; Roseboom, W.; Albracht, S. P. J.; Axley, M. J.; Scott, R. A.; Maroney, M. J. *J. Am. Chem. Soc.* **1996**, *118*, 11155–11165. (g) de Lacey, A. L.; Hatchikian, E. C.; Volbeda, A.; Frey, M.; Fontecilla-Camps, J. C.; Fernandez, V. M. *J. Am. Chem. Soc.* **1997**, *119*, 7181–7189. (h) Geßner, Ch.; Stein, M.; Albracht, S. P. J.; Lubitz, W. *JBIC* **1999**, *4*, 379–389.

* To whom correspondence should be addressed. Phone: 33-4-76-88-59-20. Fax: 33-4-76-88-51-22. E-mail: juan@lccp.ibs.fr.

[§] Institut de Biologie Structurale.

[†] Instituto de Catálisis.

[‡] Institut de Biologie Structurale et Microbienne.

(1) Albracht, S. P. J. *Biochim. Biophys. Acta* **1994**, *1188*, 167–204.

(2) Adams, M. W. W. *Biochim. Biophys. Acta* **1990**, *1020*, 115–145.

(3) Adams, M. W. W.; Mortenson, L. E.; Chen, J. S. *Biochim. Biophys. Acta* **1981**, *594*, 105–176.

(4) Krasna, A. I.; Ritemberg, D. *J. Am. Chem. Soc.* **1954**, *76*, 3015–3020.

(5) van der Zwaan, J. W.; Albracht, S. P. J.; Fontijn, R. D.; Slater, E. C. *FEBS Lett.* **1985**, *179*, 271–277.

ligand has been assigned to a sulfur species.^{8c} This oxidation is reversible, and in the reduced, active enzyme the oxo (or sulfur) ligand is missing.^{8d,e} Thus, in addition to playing a role in the redox processes, the Ni ion may protect the active site against oxygen-induced damage.

The second class of enzymes, the Fe-only hydrogenases, has been less studied. Different lines of evidence have indicated the presence of an unusual 6-Fe cluster (the H-cluster)¹¹ which has also been proposed to have CO and CN⁻ coordination.¹² The active oxidized enzyme displays the unusual $g = 2.10$ EPR signal, but subsequent reduction results in H-cluster EPR-silent species.^{2,11b,c,13} The crystal structures of the H₂-uptake enzyme from *D. desulfuricans* ATCC 7757 (DdH)¹⁴ and the H₂-evolving enzyme from *Clostridium pasteurianum* (CpI)¹⁵ have been recently solved. These studies have shown that the H-cluster is actually composed of a standard [4Fe4S] center bridged through a cysteine residue to a very unusual Fe–Fe unit.^{14,15,16} The proposed crystallographic models for the active sites of these two hydrogenases were quite similar, except for the following points (Figure 1): (1) in DdH, the two Fe centers are bridged by a small molecule, initially modeled as 1,3-propanedithiolate (PDT), and by a water molecule or some undefined arrangement of light atoms in CpI; (2) the two Fe's are further bridged by a water molecule in the former enzyme and by a CO in the latter; (3) one of the sites of the distal (relative to the [4Fe4S] cluster) Fe (Fe2) is apparently vacant in DdH but is occupied by a water molecule in CpI. We have argued¹⁶ that these differences are most likely due to a different redox state of the crystals. In the case of CpI, crystals were grown in a glovebox in the presence of dithionite under a 100% N₂ atmosphere, whereas for the crystallization of the DdH, a 10% H₂/90% N₂ atmosphere was used most of the time. It seems likely that in the former case, the crystals got oxidized, because the pH was optimal for auto-oxidation by hydrogen production, and there was a limited

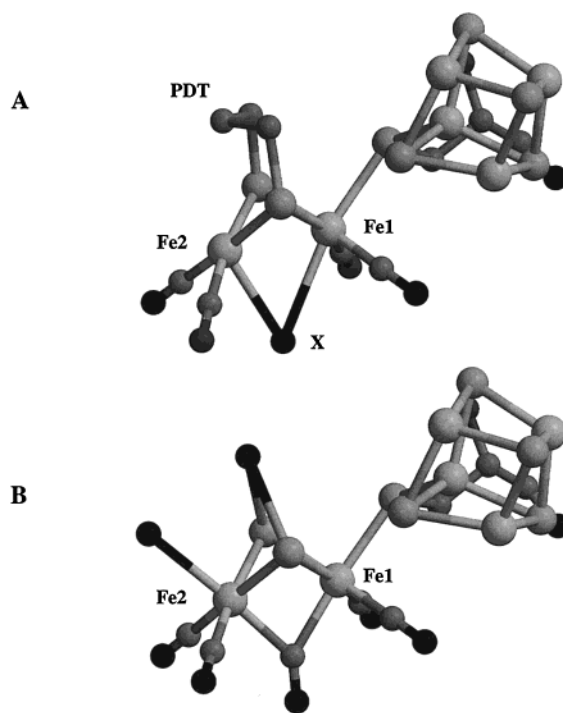


Figure 1. The crystallographic models of the active sites (H-clusters) of (a) DdH and (b) CpI. See text for model differences.

amount of dithionite added.¹⁵ For the latter, the presence of a hydrogen-containing atmosphere for most of the time resulted in a partially reduced state.

We have initiated a series of X-ray crystallographic and FTIR studies in order to better characterize the structure of well-defined redox states of the Fe-only hydrogenase from *D. desulfuricans*. Here, we report the structure of its reduced active site which has been solved at 1.85 Å resolution. On the basis of the stereochemistry around the active site, we also speculate on the nature of the central atom of its small organic molecule.

Experimental Section

Sample Preparation. The protein was purified aerobically as previously reported.^{11b,c} To obtain a homogeneous reduced crystalline enzyme the following procedure was used: (i) a 10 bar H₂ pressure was applied to the sample in solution for 2 h to activate the enzyme,^{11c} (ii) crystallization trials [2.4 M ammonium sulfate, 2.1 mM dimethyl dodecylamine-*N* oxide (DDAO), 100 mM glycine/sodium hydroxide, pH 8.8; protein concentration, 20 mg/mL] were carried out in a glovebox under a 10% H₂/90% N₂ atmosphere, and (iii) the crystals were subsequently exposed to 6 bar of H₂ pressure for 15 min prior to flash-cooling in liquid propane¹⁷ in the glovebox.

Structure Determination. Data were collected at 100 K on a single crystal to 1.85 Å resolution, at the ID14 eh3 beam line of the European Synchrotron Radiation Facility (ESRF). Initially, data were processed with the program MOSFLM¹⁸ in the orthorhombic space group $P2_12_12_1$ ($a = 116.97$ Å, $b = 130.94$ Å, $c = 131.13$ Å), giving an R_{sym} of 0.073 and 88.8% data completeness (Table 1). A molecular replacement procedure with the program AMORE¹⁹ using the 1.6 Å resolution structure previously determined as a starting search model was consistent with the crystals' containing four hydrogenase molecules per asymmetric unit. However, the crystallographic refinement of this model was blocked at R_{free} ²⁰ values of about 0.35. Subsequent careful

(17) Vernède, X.; Fontecilla-Camps, J. C. *J. Appl. Crystallogr.* **1999**, *32*, 505–509.

(18) Leslie, A. G. W. In *Crystallographic Computing*; Moras, D., Podjarny, A. D., Thierry, J. C., Eds.; Oxford University Press: New York, 1991, pp 50–61.

(19) Navaza, J. *Acta Crystallogr.* **1994**, *A50*, 157–163.

(20) Brünger, A. T.; *Nature*, **1992**, *355*, 472–474.

(8) (a) Volbeda, A.; Charon, M. H.; Piras, C.; Hatchikian, E. C.; Frey, M.; Fontecilla-Camps, J. C. *Nature* **1995**, *373*, 580–587. (b) Volbeda, A.; Garcin, E.; Piras, C.; de Lacey, A. L.; Fernandez, V. M.; Hatchikian, E. C.; Frey, M.; Fontecilla-Camps, J. C. *J. Am. Chem. Soc.* **1996**, *118*, 12989–12996. (c) Higuchi, Y.; Yagi, T.; Yasuoka, N. *Structure* **1997**, *5*, 1671–1680. (d) Garcin, E.; Vernede, X.; Hatchikian, E. C.; Volbeda, A.; Frey, M.; Fontecilla-Camps, J. C. *Structure* **1999**, *7*, 557–566. (e) Higuchi, Y.; Ogata, H.; Miki, K.; Yasuoka, N.; Yagi, T. *Structure* **1999**, *7*, 549–556.

(9) (a) Pavlov, M.; Siegbahn, P. E. M.; Blomberg, M. R. A.; Crabtree, R. H. *J. Am. Chem. Soc.* **1998**, *120*, 548–555. (b) Amara, P.; Volbeda, A.; Fontecilla-Camps, J. C.; Field, M. J. *J. Am. Chem. Soc.* **1999**, *121*, 4468–4477. (c) De Gioia, L.; Fantucci, P.; Guigliarelli, B.; Bertrand, P. *Inorg. Chem.* **1999**, *38*, 2658–2662. (d) Niu, S.; Thomson, L. M.; Hall, M. B. *J. Am. Chem. Soc.* **1999**, *121*, 4000–4007. (e) Pavlov, M.; Blomberg, M. R. A.; Siegbahn, P. E. M. *J. Quantum. Chem.* **1999**, *73*, 197–207.

(10) (a) Dole, F.; Fournel, A.; Magro, V.; Hatchikian, E. C.; Bertrand, P.; Guigliarelli, B. *Biochemistry* **1997**, *36*, 7847–7854. (b) Huyett, J. E.; Carepo, M.; Pamplona, A.; Franco, R.; Moura, I.; Moura, J. J. G.; Hoffman, B. M. *J. Am. Chem. Soc.* **1997**, *119*, 9291–9292.

(11) (a) Hagen, W. R.; van Berkel-Arts, A.; Krüse-Wolters, K. M.; Voordow, G.; Veeger, C. *FEBS Lett.* **1986**, *203*, 59–63. (b) Adams, M. W. W.; Eccleston, E.; Howard, J. B.; *Proc. Natl. Acad. Sci.* **1989**, *86*, 4932–4936. (c) Hatchikian, E. C.; Forget, N.; Fernandez, V. M.; Williams, R.; Cammack, R. *Eur. J. Biochem.* **1992**, *209*, 357–365. (d) Pierik, A. J.; Hagen, W. R.; Redeker, J. S.; Wolbert, R. B. G.; Boersma, M.; Verhagen, M. F. J. M.; Grande, H. J.; Veeger, C.; Mutsaers, P. H. E.; Sands, R. H.; Dunhan, W. R. *Eur. J. Biochem.* **1992**, *209*, 63–72. (e) Popescu, C. V.; Münck, E. *J. Am. Chem. Soc.* **1999**, *121*, 7877.

(12) Pierik, A. J.; Hulstein, M.; Hagen, W. R.; Albracht, S. P. J. *Eur. J. Biochem.* **1998**, *258*, 572–578.

(13) Patil, D. S.; Moura, J. J. G.; He, S. H.; Teixeira, M.; Prickril, B. C.; DerVartanian, D. V.; Peck, H. D., Jr.; LeGall, J.; Huynh, B. H. *J. Biol. Chem.* **1988**, *263*, 18732–18738.

(14) Nicolet, Y.; Piras, C.; Legrand, P.; Hatchikian, E. C.; Fontecilla-Camps, J. C. *Structure* **1999**, *7*, 13–23.

(15) Peters, J. W.; Lanzilotta, W. N.; Lemon, B. J.; Seefeldt, L. C. *Science* **1998**, *282*, 1853–1858.

(16) Nicolet, Y.; Lemon, B. J.; Fontecilla-Camps, J. C.; Peters, J. W. *Trends Biochem. Sci.* **2000**, *25*, 138–143.

Table 1. X-ray Data Statistics in Space Groups $P4_3$, $P2_12_12_1$ and $P1$

	space group		
	$P4_3$	$P2_12_12_1$	$P1$
R_{merge}^a	0.084 (0.253)	0.073 (0.244)	0.057 (0.228)
I/σ^b	5.8 (2.7)	6.6 (2.7)	9 (2.9)
completeness (%)	88.9	88.8 (64.9)	44.6 (23.5)
multiplicity	3.7	3.2 (2.9)	1.5 (1.7)
N_{meas}^c	598 076	522 795	487 234
N_{unique}^d	162 027	164 695	320 245

^a $R_{\text{merge}} = \sum_{hkl} \sum_j (I_{hkl} - \langle I_{hkl} \rangle) / \sum_{hkl} I_{hkl}$. ^b Signal-to-noise ratio. ^c Number of measured reflections. ^d Number of unique reflections. The statistics are given for the overall data set and for the higher resolution shell (1.9–1.85 Å) in brackets. The R_{sym} values could not be used to discriminate between $P4_3$, $P2_12_12_1$ and $P1$.

Table 2. Refinement Statistics

no. independent atoms	8383
no. independent non-protein atoms	749 waters, 2 sulfate ions, 2 Zn^{2+} , 1 DDAO, 2 cysteines, 4 glycerol molecules
resolution (Å)	10–1.85
no. reflections used for refinement	149 876
no. of reflections R_{free} calculation	7534
R factor ^a	0.171
R_{free} factor	0.183
rmsd ^b	
bonds (Å)	0.010
angles (deg)	1.6
dihedrals (deg)	23.6
torsions (deg)	0.90

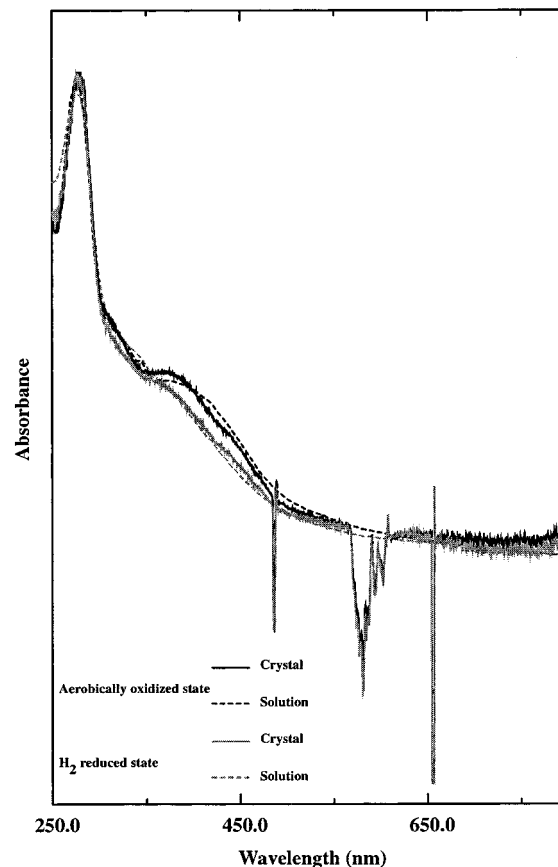
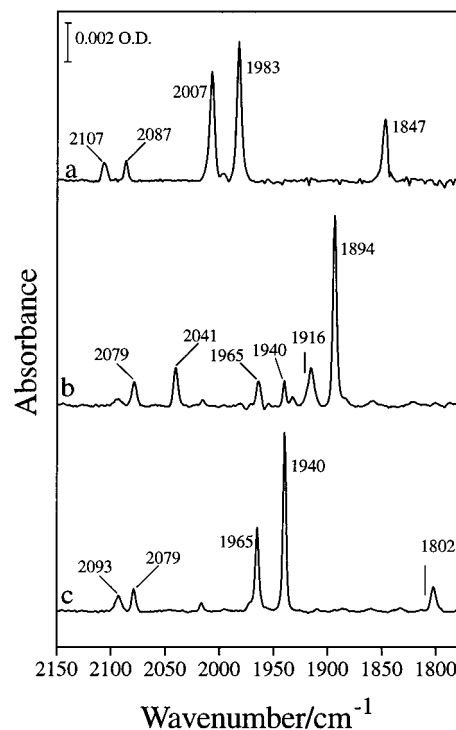
^a R factor = $\sum_{hkl} (F_{\text{obs}} - F_{\text{calc}}) / \sum_{hkl} F_{\text{obs}}$. The R_{free} factor was calculated using 5% of the reflections that were excluded during all of the refinement stages. ^b Root-mean-square deviations calculated for bond distances, angles, dihedrals and torsion angles. The four molecules in the asymmetric unit were refined as two pairs related by NCS.

examination of the electron density maps showed small deviations from $P2_12_12_1$ symmetry, which indicated that the crystal was not orthorhombic. The data were then reindexed in the space group $P1$ ($a = 116.97$ Å, $b = 130.77$ Å, $c = 130.90$ Å, $\alpha = \beta = \gamma = 90^\circ$), which resulted in a good R_{sym} but low data completeness (Table 1). The triclinic 16 noncrystallographic-symmetry (NCS) operators were then refined in $P1$ using a rigid-body procedure with the program CNS²¹ and the $P2_12_12_1$ molecular replacement solution as a starting model. The structure was subsequently refined with CNS after removing a new 5% of the reflections in order to calculate the R_{free} using the data in $P1$.²⁰ Electron density maps were recalculated after some cycles of density modification (16-fold averaging), using the program DM,²² in order to restore all of the missing structure factors and to prevent map distortions. Manual model corrections were performed using the program TURBO.²³ At all stages of the refinement, a strict 16-fold NCS was applied to the model. Six cycles of alternating refinement and manual model corrections resulted in a model with R_{free} and R_{work} factors of 0.206 and 0.204, respectively (Table 2). The validity of such a process was verified by examining the electron density map at regions of the model that were omitted during the calculation (results not shown). At this point, a new examination of the NCS operators indicated that the crystals belonged, in fact, to the tetragonal space group $P4_3$ ($a = b = 131.0$ Å, $c = 116.97$ Å). After reindexing and integration in this space group, a refinement procedure converged at an R_{work} of 0.171 and an R_{free} of 0.183 (Table 1). (The R_{free} value may be an underestimate because the initial 5% reflections taken out for its calculation using

(21) Brünger, A. T.; Adams, P. D.; Clore, G. M.; DeLano, W. L.; Gros, P.; Grosse-Kunstleve, R. W.; Jiang, J. S.; Kuszewski, J.; Nilges, M.; Pannu, N. S.; Read, R. J.; Rice, L. M.; Simonson, T.; Warren, G. L. *Acta Crystallogr.* **1998**, *D54*, 905–921.

(22) CCP4, Collaborative Computational Project Number 4. *Acta Crystallogr.* **1994**, *D50*, 760–763.

(23) Roussel, A.; Cambillau, *Silicon Graphics Geometry Partner Directory*; C. Silicon Graphics: Mountain View, CA; 1989, pp 77–78.

**Figure 2.** UV spectra of a crystal and solutions of *D. desulfuricans* (ATCC 7757) Fe-only hydrogenase.**Figure 3.** FTIR spectra of 1 mM DdH in 50 mM Hepes buffer, pH 8.0, 100 mM KCl at 25 °C in the presence of redox mediators: (a) as isolated, (b) after reduction at -535 mV, and (c) after reoxidation at -285 mV.

$P1$ were not all independent in $P4_3$). The final model is of good quality;²⁴ deviations from ideal stereochemistry are those expected from an average model refined at 1.8-Å resolution. A total of 92.8% of all

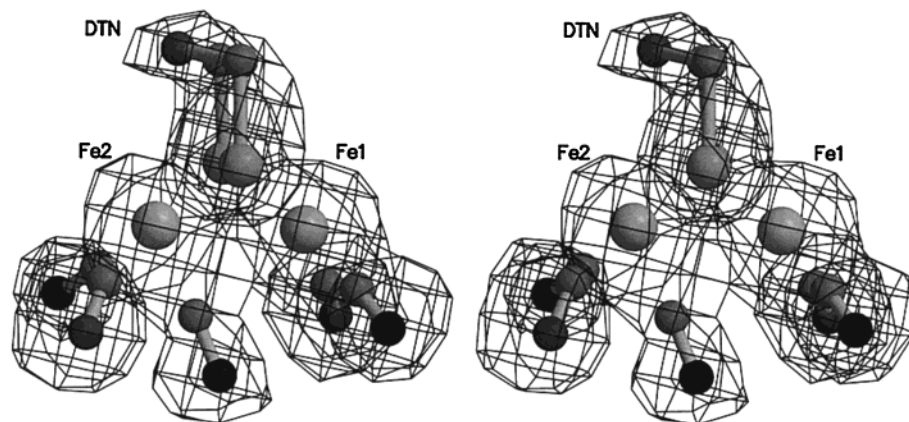


Figure 4. Stereoview of the reduced active site. The mFobs–DFcalc electron density map (SIGMAA²²) was calculated using a model in which the active-site atoms were removed from both structure factor and phase calculations. The map is contoured at the 3σ level with a cover radius of 1.7 Å. This electron density map clearly indicates that the CO that is located between the two irons is terminally bonded to Fe2. Selected distances and angles for this arrangement (noncrystallographically related molecule no. 2 in parentheses): Fe1–Fe2, 2.55 Å (2.61 Å); Fe1–C, 2.40 Å (2.56 Å); Fe2–C, 1.69 Å (1.69 Å); Fe1–O, 2.91 Å (3.12 Å); Fe2–O, 2.80 Å (2.80 Å); Fe1–C–O, 109.9° (106.4°); Fe2–C–O, 176° (178°).

of the residues has main chain torsion angles in the most favored region of the Ramachandran plot, whereas only 0.2% (1 residue) has an unfavorable ϕ – ψ combination. This residue is Glu77 from the small subunit and its ϕ – ψ angles are the same as in the initial 1.6-Å resolution structure (PDB accession code, 1HFE). Examination of the environment of Glu77 shows that this residue is located between the C-terminal region of an α -helix and the N-terminal end of a β -turn. The interactions of these two secondary structural elements with other regions of the protein are likely to compensate for the unusual torsion angles of Glu77.

FTIR Measurements. The infrared spectra were recorded in a Nicolet Magna-IR 860 Fourier transform spectrometer equipped with a MCT detector and a purge system of CO₂ and H₂O (Whatman). An IR-spectroelectrochemical cell was used as described by Moss et al.²⁵ The redox potential in the cell was controlled with a BAS CV-27 potentiostat and measured with a Fluke 77 multimeter. The temperature of the cell was controlled by a Huber CC 230 thermostat. The hydrogenase sample was concentrated by ultrafiltration with Centricon (Amicon) to 1 mM, and the FTIR spectra were measured in the presence of a mixture of redox mediators, 0.5 mM each. The redox mediators used were: indigotetrasulfonate ($E'_{\text{pH } 8} = -76$ mV, Merck), indigo carmine ($E'_{\text{pH } 8} = -159$ mV, Fluka), anthraquinone-1,5-disulfonic acid ($E'_{\text{pH } 8} = -234$ mV, ICN Pharmaceuticals), anthraquinone-2-sulfonate ($E'_{\text{pH } 8} = -277$ mV, Serva), benzil viologen ($E'_{\text{pH } 8} = -358$ mV, Sigma), methyl viologen ($E'_{\text{pH } 8} = -449$ mV, Aldrich). All redox potentials are given relative to the standard hydrogen electrode. The IR spectra were averaged from 124 scans, and the spectral resolution was 2 cm⁻¹. All spectra were blank-subtracted and baseline-corrected using the OMNIC software from Nicolet.

UV Measurements. A flash-cooled reduced crystal, prepared as described above, was transferred to a goniostat equipped with a cryogenic setup and connected to a spectrophotometer and a hydrogen lamp through fiber optics. The spectrum recorded between 250 and 750 nm is shown in Figure 2. Subsequently, the crystal was allowed to reoxidize by stopping the flow of cooled nitrogen gas (100 K) and exposing it to room-temperature air for 10 s. Equivalent experiments were carried out in solution, except that the oxidized sample was the as-prepared, aerobically-purified, enzyme.

EPR Measurements. A solution of enzyme, reduced as described above, was frozen in liquid nitrogen in an EPR tube. The CW EPR spectrum was recorded on a X-band EMX Bruker spectrometer equipped with an Oxford Instrument ESR 900 helium-flow cryostat.

Experimental conditions: T , 10 K; P , 1 mW; microwave frequency, 9.655 GHz; modulation amplitude, 1 mT.

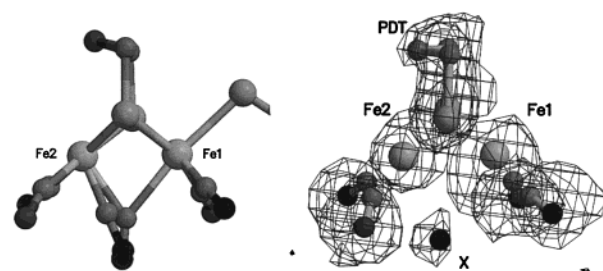


Figure 5. (A) Differences in the ligation of the bridging CO between Cpl and the reduced active site of DdH (only the bridging CO is depicted for Cpl): The CO is terminally bonded to Fe2 in the reduced DdH, and it bridges Fe1 and Fe2 in the putatively oxidized Cpl. This observation agrees well with results from FTIR spectroscopy for various redox states of DdH (see Figure 4). This superposition shows that when the CO goes from bridging to terminal, only its C atom moves significantly, which explains the observed electron density for the bridging ligand in the 1.6-Å resolution DdH structure (B).

Results and Discussion

EPR and UV Spectroscopic Evidence for the Reduction of DdH Crystals. The 350–450-nm region of the UV spectrum shown in Figure 2 clearly indicates that most, if not all, of the FeS clusters are reduced after treating the crystal as described in the Experimental Section. This is further confirmed by the spectral changes that were observed after the reoxidation experiment. Similar measurements in solution (Figure 2) and an EPR analysis of the reduced DdH solution (not shown) also indicated that the procedure used here was sufficient to reduce the enzyme both in solution and in the crystals.

The Structure of the DdH-Reduced Active Site. As in the case of the enzyme from *D. vulgaris* Hildenborough strain,¹² the FTIR spectra of different redox states of DdH (Figure 3) suggests that the active-site binuclear iron center contains two CN⁻s, two terminal COs and an additional CO ligand that seems to switch from a bridging to a terminal position upon reduction. Because the active site of Cpl has a bridging CO, we have hypothesized¹⁶ that it was in an oxidized state. This is, in fact, very likely, because Cpl crystals were grown at pH 5.1, which is optimal for auto-oxidation through hydrogen evolution, and there was only a limited amount of dithionite present.¹⁵ In the structure of the hydrogen-reduced DdH, it is very clear that the

(24) Laskowski, R. A.; MacArthur, M. W.; Moss, D. S.; Thornton, J. M. *J. Appl. Crystallogr.* **1993**, *26*, 283–291.

(25) Moss, D.; Nabdryk, E.; Breton, J.; Mantele, W. *Eur. J. Biochem.* **1990**, *187*, 565–572.

additional CO is terminally bonded to Fe2 (Figure 4). This result fully agrees with and complements those obtained from the FTIR spectroscopy experiments depicted in Figure 3. Furthermore, we think we can now provide an explanation for the shape of the electron density corresponding to the bridging ligand that was modeled as a water molecule in the previously reported 1.6-Å resolution DdH structure¹⁴ (labeled X on Figures 1 and 5B). In going from the (putatively) oxidized state, as seen in CpI, to the reduced one, as determined here for DdH, the movement of the bridging CO to a terminal position affects mostly the C atom, the O atom position being kept almost invariant (Figure 5). Consequently, a mixture of these two states in the crystal would result in electron density corresponding only to the oxygen atom of the CO molecule. This is further suggested by the Fe1-X and Fe2-X distances of about 2.6 Å, which are too long for either an oxo or a hydroxo or a water molecule ligand. In retrospect, such a result is not very surprising, because there was no controlled reduction of the aerobically prepared protein sample.

Implications of the Redox-Dependent Switch of the Bridging CO. Several lines of evidence point at Fe2 as the primary hydrogen binding site. In the partially reduced form of DdH, this iron center displays an apparently vacant site (at least a site not occupied by a non-hydrogen atom);¹⁴ in CpI, it binds the exogenous CO inhibitor;²⁶ and in both enzymes there is a hydrophobic channel that connects the molecular surface to Fe2.^{14,16} The FTIR results (Figure 3) show that in the active oxidized state (spectrum at -285 mV), there is a band at 1802 cm^{-1} which may be assigned to a bridging CO,²⁷ and that almost certainly is equivalent to the one observed in the putatively oxidized state of CpI.¹⁵ Upon reduction, this CO binds terminally to Fe2, as shown by X-ray crystallography; an observation that is confirmed by the FTIR spectroscopic results reported here. The simplest interpretation for this change is that a nearly symmetrical charge distribution at the two iron centers in the oxidized forms (as indicated by a bridging CO) becomes asymmetric when Fe2 is reduced, putatively binds a hydride, or both. A more electron-rich Fe2 favors the CO ligand transition from bridging to terminal binding, because it optimizes back-bonding from the metal to the ligand. In addition, excessive electron density may be transferred from Fe2 to Fe1 through a dative bond, and the latter can, in turn, back-donate electron density from its filled $d\pi$ orbitals to the empty π^* orbital of the C atom of the asymmetrically bound CO. These concerted electronic changes, which are aimed at mitigating the inequality in Fe ion charges, have already been proposed for a small molecule containing two Fe centers and a semi-bridging CO.²⁸ The stereochemistry of the reduced structure reported here and the FTIR spectrum of the reduced state, in which an intense band at 1894 cm^{-1} (intermediate between the frequencies of the terminal and bridging CO bands of the oxidized states) is observed, is consistent with this scheme.

Nature of the Five-Atom Fe-Bridging Molecule. As was previously observed, the electron density map around the active site clearly indicates that the two Fe's are bridged by a small molecule composed of five covalently bonded atoms.¹⁴ Although the interpretation seems unambiguous for the two sulfurs bridging Fe1 and Fe2, it is not possible to distinguish crystallographically between C, O, or N assignments for the three other

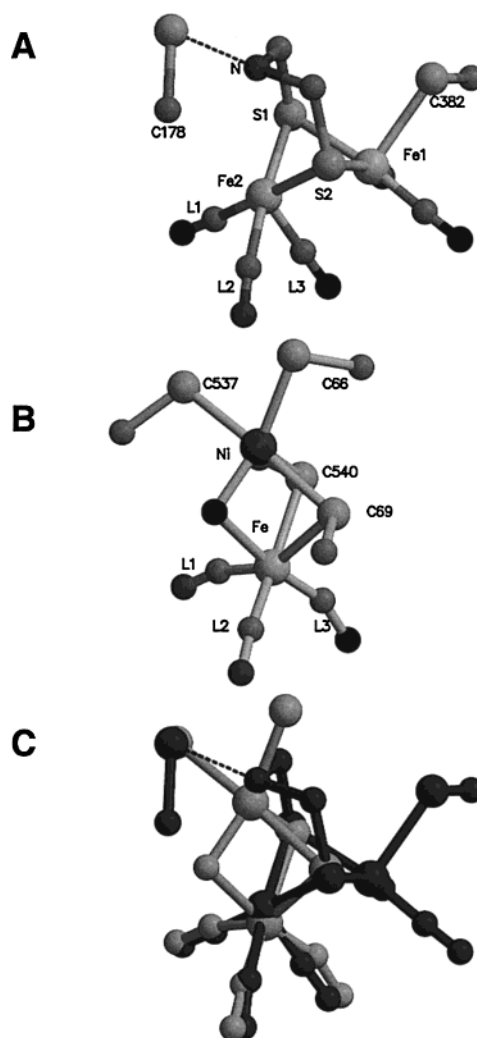


Figure 6. Comparison of the active sites of the reduced DdH (A) and the oxidized (mostly Ni-A) NiFe hydrogenase from *Desulfovibrio fructosovorans* (Montet, Y. et al. unpublished results) (B). The cysteine ligands of the active site in NiFe hydrogenase are depicted only by their C β and S atoms. The orientation of the two active sites has been chosen in order to maximize the superposition of the coordination spheres of the Fe site of the NiFe hydrogenase and the Fe2 site of the Fe-only hydrogenase (C, DdH depicted in black). Both of them are coordinated by two thiolate sulfurs (cysteines or DTN), three strong field diatomic ligands (COs and CNs; labeled L1, L2, and L3), and an apparently vacant site in DdH, occupied by a putative (hydroxo)oxo (O) ligand. In this superposition, one-half of the atoms of each active site are nearly identically placed, and the Ni atom position in the NiFe hydrogenase roughly matches that of the postulated N atom of the putative DTN in DdH.

atoms in our electron-density maps. We have now looked into this problem in greater detail: in the reduced DdH model the $S\gamma$ of Cys178 is 3.1 Å from the central atom (CA) of the small molecule that we previously modeled as PDT. This short distance and the overall stereochemistry are more compatible with a hydrogen bond than with a van der Waals contact. If CA were C as in PDT, the hydrogen bond would be of the type C-H \cdots S $^-$, which is unlikely. Furthermore, in the CO-inhibited DdH active site, the ligand's O atom lies \sim 2.5 Å from CA (our unpublished results). These two observations are not in favor of a carbon assignment for this atom. We will speculate that the most likely alternative would be N, because a central nitrogen atom would form a secondary amine that is capable of extracting the proton resulting from the heterolytic cleavage of H_2 .⁴ The protein does not seem to provide such a function,

(26) Lemon, B. J.; Peters, J. W. *Biochemistry* **1999**, *38*, 12969–12973.

(27) Nakamoto, K. *Infrared and Raman Spectra of Inorganic and Coordination Compounds, Part B*, 5th ed.; John Wiley & Sons: New York, 1997; pp 126–127.

(28) Cotton, F. A.; Wilkinson, G. *Advanced Inorganic Chemistry*, 5th ed.; John Wiley & Sons: New York, 1997; pp 1030–1031.

because the only basic residue in the active-site cavity, Lys 237, is $>4 \text{ \AA}$ away from Fe2, and in addition, it forms a salt bridge with Glu240. Our speculation is also based on the fact that a N atom different from a cyanide N was tentatively found by ESEEM to be close to active-site Fe ion(s) in both CpI^{29a} and DvH.^{29b} Consequently, we propose the small exogenous molecule to be a di-(thiomethyl)-amine (DTN), $^{-}\text{S}-\text{CH}_2-\text{NH}-\text{CH}_2-\text{S}^{-}$, not PDT as we previously suggested.¹⁴ The notion that the secondary amine of DTN could function as a base is specially attractive, because its hydrogen atom could readily switch positions through the Walden inversion, allowing proton transfer toward the S γ of Cys178 without perturbing the active-site geometry. Peters and co-workers have identified a plausible proton-transfer pathway involving the S γ of the equivalent Cys299 of CpI.¹⁵ This pathway, which extends all the way to the protein surface, is conserved in DdH.

Comparison of the Active Site of the NiFe and Fe-Only Hydrogenases. We have already indicated that there are several similarities between the active sites of Fe-only and NiFe hydrogenases: both centers are binuclear with CO, CN $^{-}$, and S coordination; they are buried in the protein core; and putative hydrophobic channels connecting the molecular surface to the active site point at apparently vacant sites of metal centers (Ni in the NiFe enzymes and Fe2 in DdH and CpI). However, no strict stereochemical equivalences were obvious when the two kinds of active site were compared.¹⁴⁻¹⁶ In the fully reduced enzyme, however, Fe2 has three terminally bound diatomic ligands, and when optimally superimposed to the Fe center of NiFe, the coordination spheres of the two ions are almost identical.³⁰ In addition to the diatomic ligands, the two bridging sulfur atoms and the vacant, potential hydride binding site occupy very similar positions (Figure 6). A remarkable consequence of this close superposition between the two active sites is that the Ni ion of NiFe enzymes and the speculative N atom of DTN occupy roughly equivalent positions (Figure 6). At this point in time, it is difficult to elaborate on this coincidence. However, it is clear that the thiolate-rich coordination of Ni and the CO/CN $^{-}$ coordination of Fe in NiFe and Fe-only hydrogenases may modulate their Lewis acid/base characteristics

(29) (a) Thomann, H.; Bernardo, M.; Adams, M. W. W. *J. Am. Chem. Soc.* **1991**, *113*, 7044-7046. (b) Van Dam, P. J.; Reijerse, E.; Hagen, W. R. *Eur. J. Biochem.* **1997**, *248*, 355-361.

(30) Although it is generally accepted that in the NiFe hydrogenases, there are two CNs and one CO and in DdH and CpI two COs and one CN, the ligand trans to the putative hydride binding site would be CO in both cases.

in ways that could make the catalytic mechanisms of the two types of hydrogenase more similar than we have previously thought.

Conclusions

In this work we report the fully reduced structure of DdH and show that the results obtained from FTIR spectroscopy are in agreement with our observations concerning changes at the enzyme's active site and that Fe2 is the most likely primary hydrogen binding site. The previously observed bridging CO ligand in CpI is now clearly terminally bound in reduced DdH. In this respect, our own previous results concerning the Fe bridging ligand of this enzyme are most likely the consequence of a mixture of anaerobically oxidized and reduced states. From both stereochemical and mechanistic considerations, we now believe that our original assignment of the small molecule that binds the binuclear Fe center as PDT was not correct. A DTN assignment, although clearly speculative, seems to make more sense to us because it contributes a base that appears to be essential for the heterolytic cleavage of hydrogen. Furthermore, when the reduced DdH active site structure is compared to the equivalent region in the NiFe hydrogenases, a remarkable similarity is found in the coordination spheres of respective Fe centers, including a coincidence between the putative N atom of DTN and the Ni center. The implications of this latter observation are not immediately obvious and may deserve further investigation.

Efforts to obtain well-diffracting oxidized crystals of DdH, either aerobically or anaerobically, are under way.

Acknowledgment. This work was partially supported by the BIO4-98-0280 grant from the European Union BIOTECH program. We thank Wim Burmeister for help with data collection at the ID14-eh3 beamline of the European Synchrotron Radiation Facility, Dominique Bourgeois for use of his "cryo-bench" for UV measurements, and J. Gaillard for the EPR measurements.

Note Added in Proof. H.J. Fan and M.B. Hall (personal communication) have carried out density function theory (DFT) calculations which indicate that a central N atom in the small organic molecule of the active site provides a low energy barrier and a stable product for the hydrogen heterolytic cleavage (or formation) reaction.

JA0020963